

Dose-dependent effects of a brain-penetrating iduronate-2-sulfatase on neurobehavioral impairments in mucopolysaccharidosis II mice

Hideto Morimoto,¹ Hiroki Morioka,¹ Atsushi Imakiire,¹ Ryuji Yamamoto,¹ Tohru Hirato,¹ Hiroyuki Sonoda,¹ and Kohtaro Minami¹

¹Research Division, JCR Pharmaceuticals, 2-2-9 Murotani, Nishi-ku, Kobe 651-2241, Japan

Deposition of heparan sulfate (HS) in the brain of patients with mucopolysaccharidosis II (MPS II) is believed to be the leading cause of neurodegeneration, resulting in several neurological signs and symptoms, including neurocognitive impairment. We recently showed that pabinafusp alfa, a blood-brain-barrier-penetrating fusion protein consisting of iduronate-2-sulfatase and anti-human transferrin receptor antibody, stabilized learning ability by preventing the deposition of HS in the CNS of MPS II mice. We further examined the dose-dependent effect of pabinafusp alfa on neurological function in relation to its HS-reducing efficacy in a mouse model of MPS II. Long-term intravenous treatment with low (0.1 mg/kg), middle (0.5 mg/kg), and high (2.0 mg/kg) doses of the drug dose-dependently decreased HS concentration in the brain and cerebrospinal fluid (CSF). A comparable dose-dependent effect in the prevention of neuronal damage in the CNS, and dose-dependent improvements in neurobehavioral performance tests, such as gait analysis, pole test, Y maze, and Morris water maze, were also observed. Notably, the water maze test performance was inversely correlated with the HS levels in the brain and CSF. This study provides nonclinical evidence substantiating a quantitative dose-dependent relationship between HS reduction in the CNS and neurological improvements in MPS II.

INTRODUCTION

Mucopolysaccharidosis II (MPS II, Hunter syndrome), an X-chromosome-linked recessive disease, is caused due to the deficiency of the lysosomal enzyme iduronate-2-sulfatase (IDS), leading to the accumulation of its undigested glycosaminoglycan substrates, namely heparan sulfate (HS) and dermatan sulfate (DS) throughout the body.^{1,2} Disease severity of MPS II varies depending on the type of mutation in the *IDS* gene: large deletions or frameshift mutations can cause a complete loss of enzyme activity, resulting in severe forms of the disease with rapidly progressive neurocognitive impairment, while the point mutations with partial loss of enzyme activity may lead to attenuated forms of the disease with little or no neurocognitive impairment.²⁻⁵ As for the treatment, enzyme replacement therapy (ERT) with recombinant human IDS (rhIDS) has been approved for use in patients with MPS II,^{6,7} while the conventional intravenous ERT is ineffec-

tive for the treatment of symptoms in the CNS because the blood-brain barrier (BBB) prevents delivery of the enzyme to the brain parenchyma. Although intrathecal or intracerebroventricular administration of rhIDS may address some CNS manifestations in MPS II, patients require implantation of a device for injection and inevitably require concomitant intravenous ERT for somatic symptoms.^{8,9}

Recently, a BBB-penetrating IDS enzyme, pabinafusp alfa (JR-141, IZCARGO[®]), was approved in Japan to treat patients with all forms of MPS II. Pabinafusp alfa is a fusion protein consisting of a humanized anti-human transferrin receptor (hTfR) antibody and human IDS, designed to be delivered to the brain parenchyma upon intravenous administration and is anticipated to reduce accumulated substrate concentrations in both the peripheral and CNS organs.¹⁰⁻¹² A nonclinical study showed that the clearance of deposited HS in the brain by long-term treatment with pabinafusp alfa prevented neurodegeneration and stabilized learning ability in a mouse model of MPS II.¹¹ Mice treated with rhIDS demonstrate a substrate reduction in somatic tissues and organs; however, neither a reduction of the substrate in the brain and CSF nor an improvement in neurohistopathological parameters or neurological manifestations was observed.¹¹ In addition, the HS concentration in the cerebrospinal fluid (CSF) was found to correlate well to HS concentration in the brain.^{11,13} Clinical trials conducted in Japan and Brazil confirmed the proof-of-concept whereby pabinafusp alfa decreased the HS concentration in the CSF and positively affected neurocognitive development in patients with MPS II.¹⁴⁻¹⁷ Longer observations are needed further to solidify the effect of pabinafusp alfa on neurological manifestations. In this context, utilization of HS concentration in the CSF as a surrogate endpoint of drug efficacy against CNS disorders in MPS II is worth considering for the early assessment of the treatment response.

Our previous nonclinical study of pabinafusp alfa demonstrated a correlation between the reduction of HS concentration in the CSF

Received 17 February 2022; accepted 6 May 2022;
<https://doi.org/10.1016/j.omtm.2022.05.002>.

Correspondence: Kohtaro Minami, Research Division, JCR Pharmaceuticals, 2-2-9 Murotani, Nishi-ku, Kobe 651-2241, Japan.

E-mail: minami-k@jp.jcrpharm.com



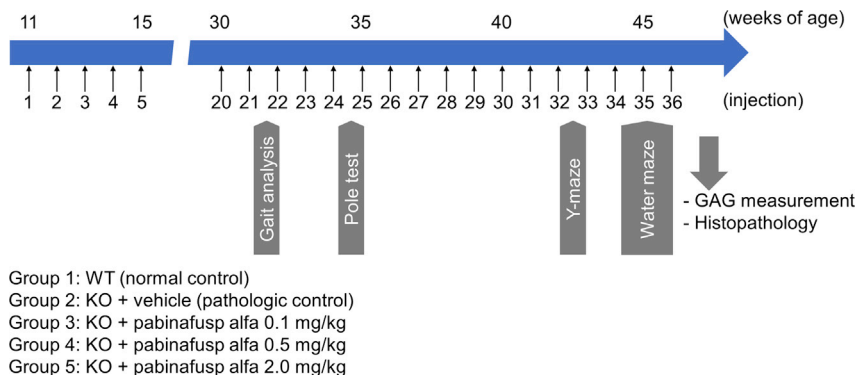


Figure 1. Schematic representation of the study schedule

WT and hTFR-KI/*ds*-KO (KO) mice ($n = 15/\text{group}$) were used in this study. Pabinafusp alfa or vehicle was intravenously injected to the mice once weekly for 36 weeks (from 11 to 46 weeks of age). The five study groups were as follows: WT (group 1), vehicle-treated KO (group 2), 0.1 mg/kg of pabinafusp alfa treated (group 3), 0.5 mg/kg of pabinafusp alfa treated (group 4), and 2.0 mg/kg of pabinafusp alfa treated (group 5). Gait analysis, pole test, and Y maze test were performed after the 21st, 24th, and 32nd injection, respectively. For the Morris water maze test, half of the animals in each group were subjected to the test after the 34th injection, and the other half were subjected to the test after the 35th injection. Tissue sampling for glycosaminoglycan (HS and DS) measurement and histopathological analysis was carried out 1 week (8 days) after the last dose. GAG, glycosaminoglycans.

and prevention of neurobehavioral impairments¹¹; however, the study did not fully substantiate a dose-dependent relationship between the decrease in the biomarker (HS concentration in the CSF) and the effect of pabinafusp alfa on neurocognitive function using the doses chosen in the study. Therefore, the present study aimed to establish a dose-dependent relationship between neurological amelioration and the reduction of HS concentration quantitatively in the CNS of a mouse model of MPS II.

RESULTS

Pabinafusp alfa dose-dependently reduced substrate concentrations in MPS II mice

We previously demonstrated the brain delivery of intravenously injected pabinafusp alfa (JR-141) in mice and monkeys.¹⁰ A dose-dependent increase in the brain distribution of the enzyme was also confirmed (Figure S1). After administering three different doses of pabinafusp alfa intravenously to MPS II mice once weekly for 36 weeks (Figure 1), the lower dose (0.1 mg/kg) barely affected the HS concentration, the middle dose (0.5 mg/kg) partially decreased its concentration, and the higher dose (2.0 mg/kg) nearly normalized the HS concentration in the CNS tissues (brain and CSF) (Figures 2A and 2B), demonstrating a dose-dependent effect of pabinafusp alfa on HS deposition in the CNS. The results were similar in the peripheral tissues, where pabinafusp alfa exerted a dose-dependent effect on HS reduction (Figures 2C–2F), which was more effective than in the CNS tissues, presumably due to more distribution of the drug in these peripheral tissues than in the CNS.^{10,12} Likewise, concentrations of DS in the peripheral tissues also decreased in a dose-dependent manner following treatment with pabinafusp alfa (Figure S2).

Pabinafusp alfa dose-dependently prevented neurohistopathological changes in MPS II mice

Neurohistopathological changes in the brain were examined by H&E staining and immunostaining for lysosomal-associated membrane protein 1 (Lamp1), glial fibrillary acidic protein (Gfap), and CD68. All these analyses were performed 1 week after the last dosing. Vacuolation and swelling of neuronal cells were commonly observed in

distinct brain regions of vehicle-treated MPS II (knockout [KO]) mice by H&E staining. The low dose (0.1 mg/kg) of pabinafusp alfa exerted no or a low effect on these pathological changes while being modestly affected at the middle dose (0.5 mg/kg) (Figures 3 and S3; Table S1). Moreover, the high dose (2.0 mg/kg) of the drug completely suppressed these pathological changes in most of the brain regions of MPS II mice (Figures 3 and S3; Table S1), as evidenced by the quantitative scoring system applied (Figures 3 and S3, right).

An increase in the immunoreactivity of Lamp1 is considered an indication of lysosomal storage of undigested materials and hypertrophy.^{18–20} While an increase in Lamp1 staining in the brain of the pathologic control (KO) mice was observed, treatment with pabinafusp alfa dose-dependently attenuated the intensity, which almost normalized at the high dose (2.0 mg/kg) in most regions (Figures 3 and S4; Table S1).

Glial activation was examined by immunostaining for Gfap and CD68. While Gfap-positive cells were scarce or not seen in the cerebral cortex, interbrain, midbrain/pons, and medulla oblongata of wild-type (WT) mice, their numbers increased in vehicle-treated MPS II (KO) mice (Figure 3 and S5; Table S1), suggesting the infiltration of astrocytes into these brain regions and the presence of neuroinflammation. Glial cell activation was suppressed by treatment with pabinafusp alfa in a dose-dependent manner and was completely blocked at the high dose (2.0 mg/kg) (Figures 3 and S5; Table S1). CD68-positive, vacuolated microglia were commonly found in all brain regions examined in vehicle-treated MPS II (KO) mice (Figures 3 and S6; Table S1), further indicating activation of glial cells and degeneration of microglia. Vacuolated microglia were barely detected in the brains of mice treated with pabinafusp alfa at the middle (0.5 mg/kg) and high (2.0 mg/kg) (Figures 3 and S6; Table S1).

The dose-dependent effects of pabinafusp alfa on these histopathological changes were consistent with the dose-dependent reduction of HS in the CNS.

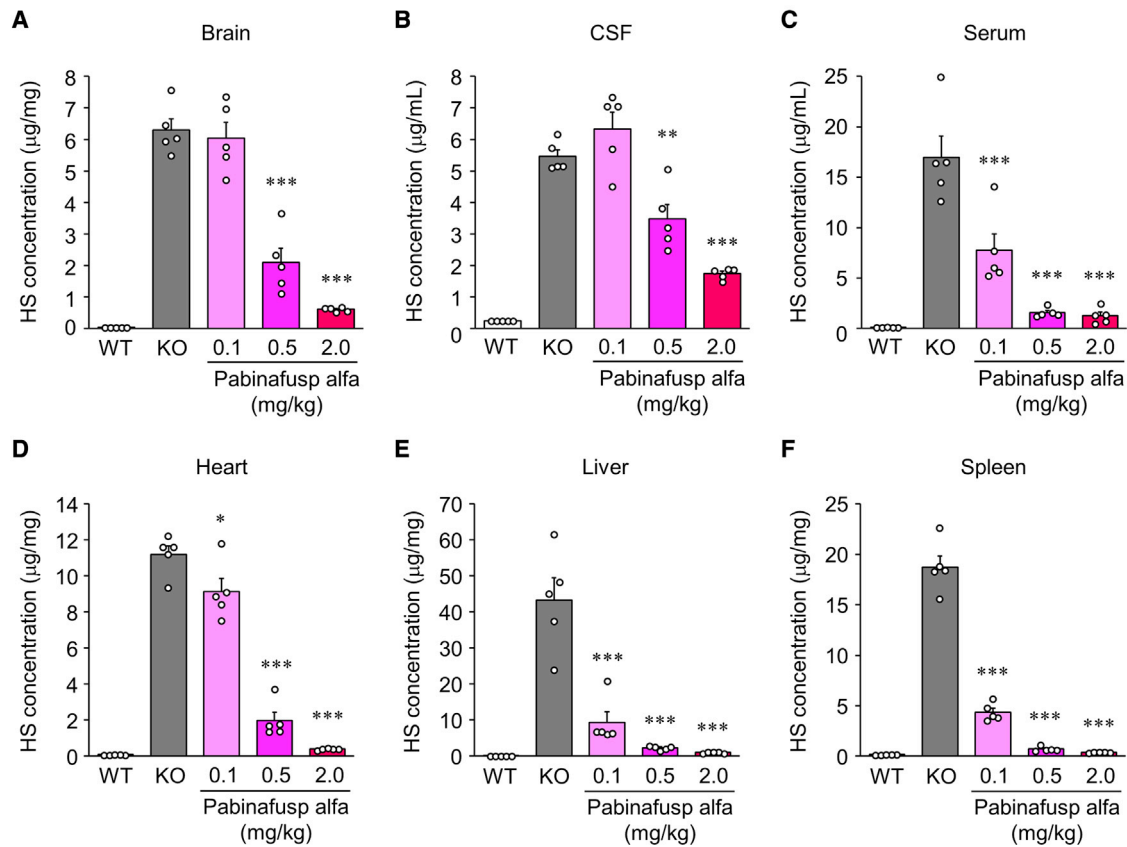


Figure 2. Dose-dependent reduction of HS concentrations in MPS II mice treated with pabinafusp alfa

Eleven-week-old MPS II mice received weekly intravenous administration of pabinafusp alfa for 36 weeks. HS concentrations were measured in the brain (A), CSF (B), serum (C), heart (D), liver (E), and spleen (F) 1 week (8 days) after the last dose. Values are means with SEM (n = 5). Results of detailed statistical analysis are shown in Table S2. *p < 0.05, **p < 0.01, ***p < 0.001 versus KO control (Dunnett's test). KO, vehicle-treated MPS II mice.

Pabinafusp alfa dose-dependently ameliorated neurological defects in MPS II mice

Next, we examined multiple neurological domain tests to assess the effects of pabinafusp alfa on motor coordination, memory, and learning deficits in MPS II mice. Initially, overall motor coordination was evaluated by gait analysis using the CatWalk XT automated system after the 21st injection (as shown in Figure 1). Compared with WT mice, vehicle-treated MPS II (KO) mice tended to decrease the average walking speed (Figure 4A), exhibiting a significant decrease in the number of steps per second (cadence, Figure 4B). The ground periods (stand) of both forelimbs and hindlimbs, and the on-air period (swing) of forelimbs but not hindlimbs significantly increased in vehicle-treated MPS II (KO) mice (Figures 4C–4F). Together with the footprint analysis (Figure S7), the MPS II mice demonstrated impaired motor coordination. Dose-dependent improvement in these gait parameters, and normalized motor coordination at the high dose (2.0 mg/kg) was seen after chronic treatment of the mice with pabinafusp alfa (Figures 4A–4F).

Motor coordination (and agility) was also examined using a pole test after the 24th injections (Figure 1). The time taken to descend the pole

was significantly longer in the vehicle-treated MPS II (KO) mice than in the WT mice (Figure 4G). However, the descending time was shortened by treatment with pabinafusp alfa in a dose-dependent manner (Figure 4G), indicating a suppression of the loss of motor coordination and agility in MPS II mice.

Immediate working memory was assessed by spontaneous alterations in the Y maze test as a neurogenic process after the 32nd injection (Figure 1). The total number of arm entries, representing spontaneous motor activity, was not significantly different between WT and KO groups (p = 0.570, t test) (Figure 5A). However, the rate of spontaneous alterations decreased in vehicle-treated MPS II (KO) mice compared with WT mice (Figure 5B), indicating an impaired working memory.²¹ The spontaneous alterations were recovered in a dose-dependent manner by pabinafusp alfa and normalized at the high-dose (2.0 mg/kg) drug level (Figure 5B), concluding that the drug prevented the loss of immediate working memory in MPS II mice.

As a final test, after the 34th injection of pabinafusp alfa, the mice were subjected to the Morris water maze test for assessing spatial

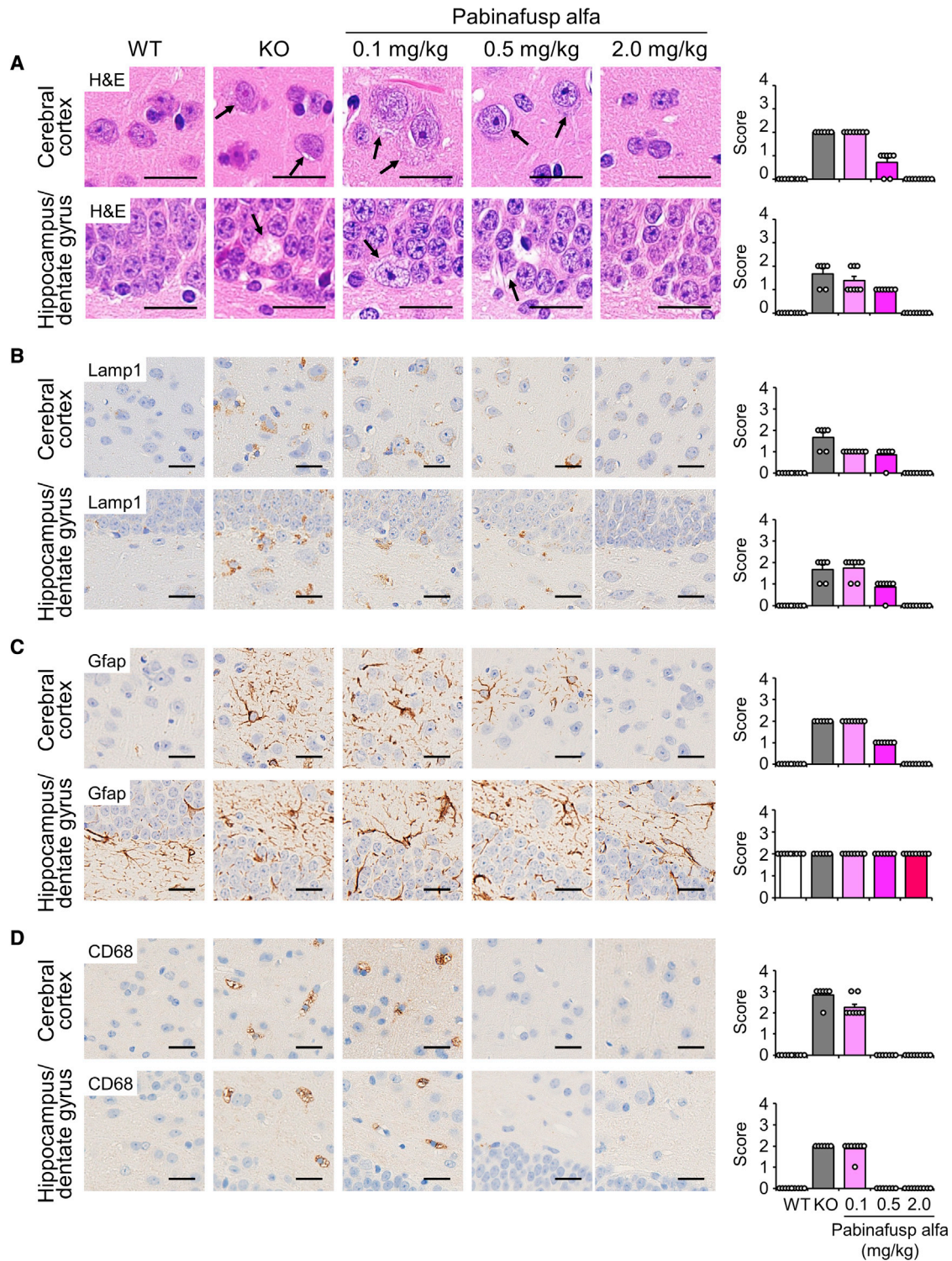


Figure 3. Dose-dependent prevention of histopathological changes in the brain

Representative photomicrographs of H&E-stained (A), Lamp1-immunostained (B), Gfap-immunostained (C), and CD68-immunostained (D) brain sections are shown. Arrows (A) (H&E staining) indicate vacuolation or swelling of neuronal cells. Brown signals (B–D) (immunostainings) indicate immunopositive cells for Lamp1 (B), Gfap (C), or CD68 (D). Graphs on the right are group means with SEM (n = 6–10) and individual scores of histopathological findings. The changes are scored as negative (0), minimal (1), mild (2), moderate (3), or severe (4). Scale bars, 20 μ m. KO, vehicle-treated MPS II mice. See also [Figures S3–S6](#).

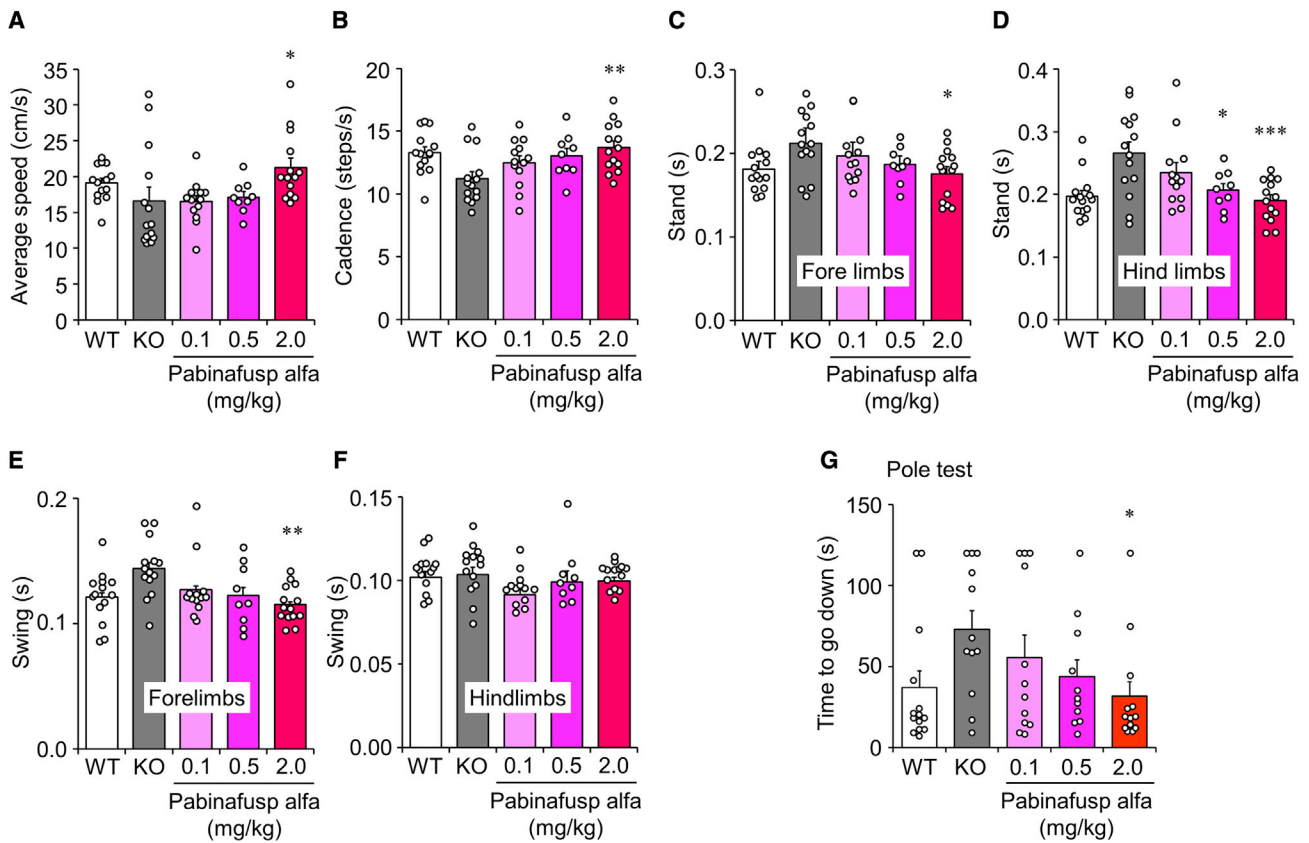


Figure 4. Dose-dependent effects of pabinafusp alfa on motor coordination and agility

(A–F) Gait dynamics were examined using the CatWalk XT automated gait analysis system after the 21st dose to assess overall motor coordination. (A) Average walking speed. (B) Cadence, representing the number of steps per second. (C and D) Stand, representing the ground period of the fore (C) or hind (D) limbs. (E and F) Swing, representing the on-air period of the fore (E) or hind (F) limbs. (G) The pole test was performed after the 24th dose to assess motor coordination and agility. Values are means with SEM ($n = 9–14$ for gait analysis and $n = 11–14$ for pole test). Results of detailed statistical analysis are shown in Table S2. * $p < 0.05$, ** $p < 0.01$, *** $p < 0.001$ between KO and each treatment group (Dunnett's test). KO, vehicle-treated MPS II mice.

learning ability. Compared with WT mice, vehicle-treated MPS II (KO) mice showed a longer goal latency (the time to reach the platform) in finding the hidden platform; the goal latency was only slightly shortened after 5 days of trials (Figure 6A), indicating an impairment in spatial learning ability. The trajectories of the mean values of the goal latency of the mice treated with the low dose (0.1 mg/kg), and the middle dose (0.5 mg/kg) of pabinafusp alfa showed mild improvement compared with that of vehicle-treated MPS II (KO) mice (Figure 6A). Mice treated with the high dose (2.0 mg/kg) of pabinafusp alfa showed learning ability comparable with WT mice (Figure 6A). The performance of individual mice in the Morris water maze test was classified as good, fair, and poor, based on the goal latency response of WT and vehicle-treated MPS II (KO) mice on trial day 5 (criteria of the performance is shown in Figure S8). As a result, most mice treated with vehicle (KO) or the low dose (0.1 mg/kg) of pabinafusp alfa were classified as poor performers (8/11 and 10/13 for KO and 0.1 mg/kg groups, respectively), a few as fair performers (3/11 and 3/13), but none as good performers (Figure 6B). In the middle-dose (0.5 mg/kg) group, two mice showed good

performance while decreasing the proportion of poor performers (8/13) compared with those in vehicle-treated (KO) or low-dose group (Figure 6B). Notably, most animals in the high-dose (2.0 mg/kg) group were good (7/14) or fair performers (3/14), similar to the WT group (Figure 6B), indicating that pabinafusp alfa treatment almost completely preserved the spatial learning ability in a mouse model of MPS II.

Association of the learning ability with HS concentration in the CNS

To understand the relationship between neurobehavioral performance and HS concentrations in the CNS, the performance in the Morris water maze test was scored as 1 (poor), 2 (fair), and 3 (good). The average score of each treatment group was plotted against the average concentration of HS in the brain or CSF of the corresponding group. The correlations (brain HS versus performance score and CSF HS versus performance score) were well fitted with nonlinear least-squares regression curves (Figures 6C and 6D). These results demonstrate the correlation of HS concentration in the CNS with

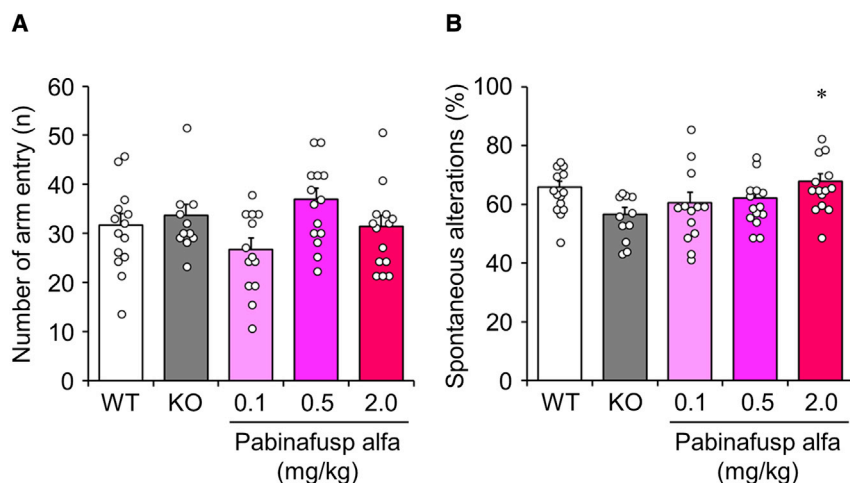


Figure 5. Dose-dependent effects of pabinafusp alfa on immediate working memory

The Y maze test was performed after the 32nd dose to assess immediate working memory. (A) Total number of arm entries representing spontaneous motor activity. There was no statistically significant difference between WT and KO control groups (t test) or between KO control and pabinafusp-alfa-treated groups (Dunnett's test). (B) Rate of spontaneous alterations representing the immediate working memory. Values are means with SEM for (n = 11–14). Results of detailed statistical analysis are shown in Table S2. *p < 0.05 between KO and the treatment group (Dunnett's test). KO, vehicle-treated MPS II mice.

the neurological performance in MPS II mice treated with the BBB-penetrating IDS fusion protein.

DISCUSSION

In general, biomarkers can provide an easy and effective way to predict disease severity and therapeutic response.²² It is critical for patients with severe MPS II to relate biomarker levels to long-term clinical outcomes of CNS function. In this respect, CSF HS, a major molecule derived from lysosomal storage materials in the CNS, is a promising candidate as a biomarker for neuronopathic MPS II. Dysfunction or loss of the lysosomal enzyme IDS causes a pathological accumulation of its substrates HS and DS in the cells throughout the body. HS accumulation in the brain is anticipated to be particularly associated with the development of neurocognitive impairments in several types of MPS, including types I, II, IIIA, IIIB, and VII.^{11,23–27} Excessive substrate accumulation in neurons impairs autophagy, organelle function, dendrite formation, axonal transport, and calcium storage.^{26–30} Astroglia and microglia are activated by the secondary accumulation of gangliosides, leading to neuroinflammation and subsequent neurodegeneration.^{31–33} Although these processes that cause clinical CNS manifestations in MPS II are undoubtedly evoked by deposition of HS in glial and neuronal cells, complexity and interdependency of the multistep pathogenic processes make it challenging to directly correlate HS levels to the resulting CNS disease severity, particularly at the quantitative level.

Therefore, the current study aimed to provide nonclinical evidence for deriving a quantitative dose-dependent relationship between HS concentration in the CSF (as a biomarker) and neurological performance using MPS II mice treated with the BBB-penetrating IDS enzyme pabinafusp alfa. We previously reported that HS levels in the CNS were related quantitatively to the dosage of pabinafusp alfa in a 12-week repeated administration study of MPS II mice,¹¹ which was also confirmed in the present study after 36-week continuous treatment at three different dose levels. The dosages of pabinafusp alfa in the current study were set to exert a clear difference in HS-

reducing efficacy in the CNS. As a result, the low dose (0.1 mg/kg) barely influenced, the middle dose (0.5 mg/kg) partially reduced, and the high dose (2.0 mg/kg) nearly normalized HS levels in the brain and CSF. Under these conditions, neurobehavioral and neurocognitive parameters in multiple domains (motor coordination, agility, immediate working memory, and spatial learning ability) showed similar dose-dependent improvements in substrate reduction. We previously demonstrated that conventional ERT with rhIDS could reduce the levels of its substrates in somatic tissues and organs but not in the CNS, thus failing to prevent neurodegenerative changes or multisymptomatic neurological impairment in MPS II mice.¹¹

The assessments of neurological manifestations were inevitably affected by changes in peripheral motor function, which may be associated with drug efficacy on skeletal abnormalities observed in MPS II mice. Because early treatment with rhIDS in patients with MPS II results in increased height and weight³⁴ and another TfR-targeting fusion protein of IDS improves skeletal phenotype in MPS II mice,³⁵ it is likely that pabinafusp alfa also has beneficial effects on skeletal dysplasia. In such cases, the improvement of neurobehavioral performance by pabinafusp alfa shown here may be at least partially accounted for by amelioration in the bone or muscular involvement. For the results obtained from the gait analysis and pole test, it may be difficult to exclude an effect on skeletal abnormalities completely. However, in the Y maze test, the total number of arm entries did not differ between the groups (Figure 5A), demonstrating that spontaneous motor activity was not altered by treatment with pabinafusp alfa. Thus, an influence of skeletal effect on the working memory performance test is highly unlikely, and the normalization of working memory by pabinafusp alfa at a high dose must be assigned to its effect on neuronal tissues, that is, the reduction of damage to the brain by clearance of HS. Nevertheless, further studies are needed to evaluate the effects of pabinafusp alfa on any skeletal abnormalities.

Regarding the Morris water maze test, it may be possible that swimming ability influences goal latency. However, we confirmed that swimming speed was not different between WT and KO mice (Figure S9). In addition, although the goal latency of KO mice on the first day (before the learning period) seemed slightly longer than that of

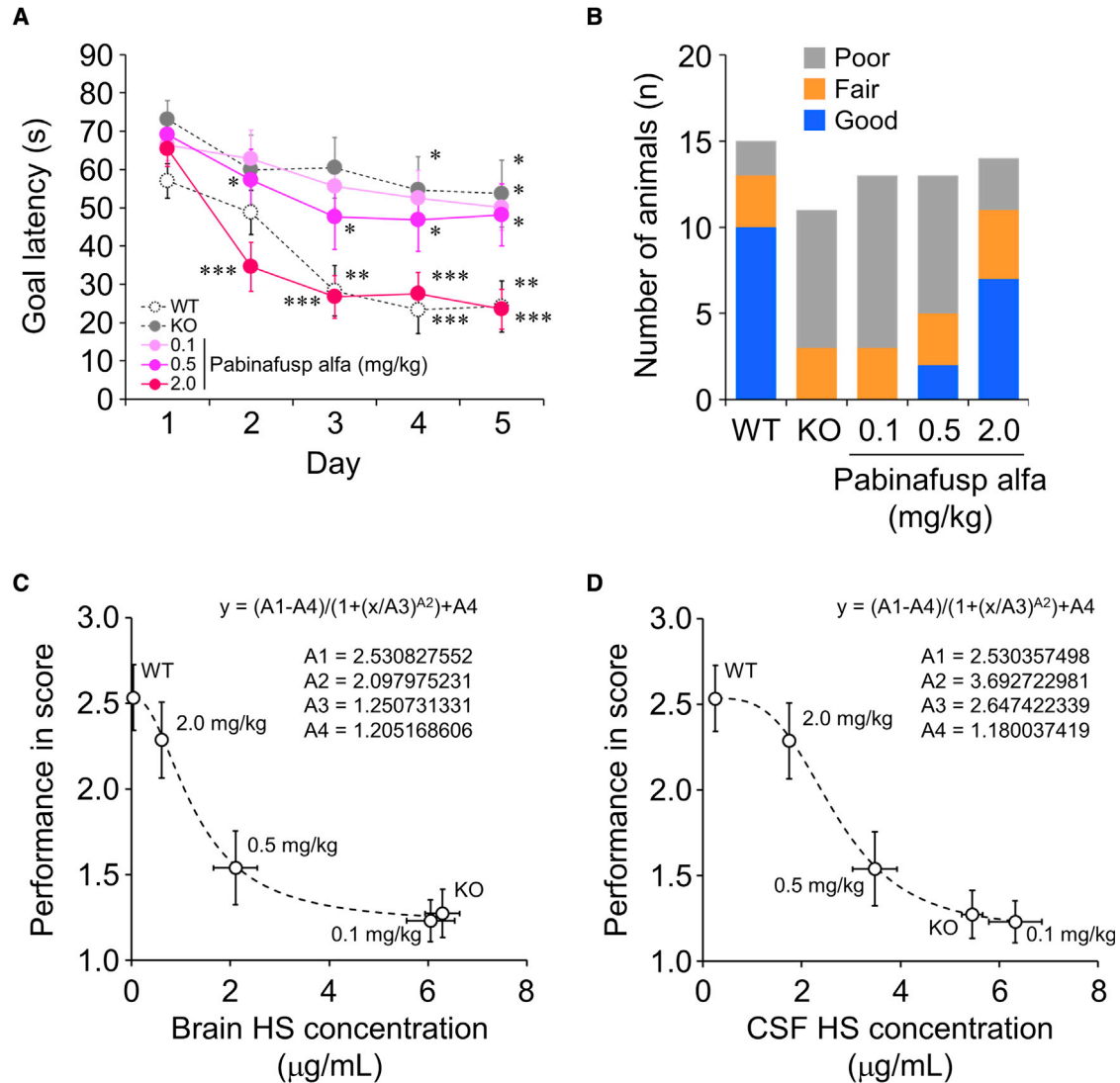


Figure 6. Spatial learning ability assessed by Morris water maze test

The Morris water maze test was performed after the 34th dose (half of the mice in each group) and the 35th dose (the remaining half of the mice in each group). (A) Goal latency. The goal latency was measured three times per day, and the means were calculated within each day for individual animals. Values are means \pm SEM ($n = 11-15$). ** $p < 0.01$, *** $p < 0.001$ versus day 1 within each group (paired t test). (B) Classification of performance in the water maze test (goal latency) on day 5. Good: < 16.81 s, fair: $16.81-30.57$ s, and poor: > 30.57 s. The criteria were determined as described in Figure S8. (C) Correlation of the performance scores with brain HS concentration. (D) Correlation of the performance score with CSF HS concentration. The performance in the Morris water maze test was scored as 1 (poor), 2 (fair), and 3 (good). The mean HS concentrations in the brain (C) and CSF (D) of each group (with SEM) were plotted against the mean performance score of the corresponding group in the water maze test (with SEM). The curves were fitted using nonlinear least-squares regression, as indicated in the figures. KO, vehicle-treated MPS II mice.

WT mice, the difference was not statistically significant (Figure 6A). In this situation, the goal latency was declining markedly day by day in the WT group while being relatively stable in the KO group during the 5-day learning period, indicating that this test system was suitable for assessing spatial learning/memory ability in the 5-day consecutive trial. Moreover, because the differences in the baseline goal latency (on day 1) between KO and pabinafusp-alfa-treated groups were not significant (Figure 6A), the influence of the altered peripheral motor function by the drug treatment was minimal on the performance

of the water maze test under the conditions used, concluding that the effect of pabinafusp alfa on the goal latency was largely accounted for by the recovery from CNS damage in the neurological assessment.

The dose-dependent effects of pabinafusp alfa on histopathological changes were highly consistent with the dose-dependent reduction in HS concentrations in the CNS. Neurodegeneration (vacuolation/swelling of neural cells) occurred in a wide region of the brain of vehicle-treated MPS II (KO) mice and was also frequently found in

the low dose (0.1 mg/kg) group with high HS levels. The middle dose (0.5 mg/kg) partially reduced HS concentrations in the CNS and also partially suppressed the histopathological neurodegeneration, while the high dose (2.0 mg/kg) nearly normalized HS concentrations and almost completely suppressed histopathological neurodegeneration. In addition to neurons, glial cells are considered to be involved in the neuropathogenesis of MPS II in the CNS.^{32,33} Glial activation and gliosis, a hallmark of neuroinflammation, were apparent in vehicle-treated MPS II mice, and infiltration of Gfap-positive astrocytes and CD68-positive vacuolated microglia were frequently found in the brain. These changes were attenuated by pabinafusp alfa in a dose-dependent manner. Together with the data from Lamp1 staining, these results demonstrate a clear association between the suppression of neuroinflammation/neurodegeneration and reduction of HS concentrations in the CNS and provide a critical link between substrate reduction and improvement in neurological manifestations in pabinafusp-alfa-treated MPS II mice.

The limitations of this study include the fact that the treatment started at an early stage (11 weeks of age) in disease progression without overt phenotypes, except for substrate accumulation. Although it is obvious that early treatment initiation is important to avoid the progression of disorders, including CNS involvement in patients with MPS II,³⁶ not all patients can be diagnosed at an early stage; thus, studies examining the possibility of restoring pathological manifestations of the disease as well as the expansion of newborn screening must be considered. Because our data from young MPS II mice showed that glial activation was observed as early as 8 weeks of age (unpublished observations), at least some of the early pathologic changes such as neuroinflammation are reversible by treatment with BBB-penetrating ERT.

The issue to address at the next step is how these nonclinical findings can be generalized and utilized in clinical studies. Previous clinical trials¹⁴⁻¹⁶ have demonstrated that pabinafusp alfa reduces HS concentration in the CSF, with either an improvement (younger patients) or stabilization (patients beyond toddlers of infant age) of cognitive development. Owing to the safety and benefit/risk ratio, it is prohibitive to collect brain tissue samples from human trial participants. Here, we demonstrated similar dose-dependency of pabinafusp alfa in reducing substrate in the CNS, ameliorating neurohistopathological changes, and neurological improvement in multiple domains in MPS II mice. Intriguingly, the decrease in HS concentrations in the CNS correlated well to neurological improvement. Thus, this study provides strong nonclinical evidence to establish a quantitative dose-dependent relationship between HS reduction in the CNS and neurological improvement in MPS II. Given that CSF collection is an acceptable clinical procedure for most patients with MPS II, utilization of HS concentration in the CSF as a surrogate endpoint is plausible and practical in neuronopathic MPS II for the early assessment of BBB-penetrating ERT response. The theory of the use of CSF HS as a biomarker may be extended to other mucopolysaccharidoses where HS is the major substrate accumulated in the CNS.

MATERIALS AND METHODS

Test substance

Pabinafusp alfa (JR-141), a genetically engineered protein consisting of a humanized hTfR antibody fused with human IDS with identical amino acid sequence to that of idursulfase (ELAPRASE[®], Sanofi), was produced in CHO cells cultured in a serum-free medium, as reported.¹⁰ The calculated molecular weight of pabinafusp alfa was 265,110.93 Da. The purified recombinant protein was stored at -80°C until use.

Animals

The murine model of MPS II used in this study was an hTfR knockin/*Ids* KO (hTfR-KI/*Ids*-KO) mouse with a C57BL/6 background.^{10,37} *Ids*-KO mice were generated by deletion of exons 2–5 from the *Ids* gene.³⁷ Because pabinafusp alfa recognizes hTfR but not murine TfR, hTfR-KI mice were produced. To produce these, a cDNA encoding a chimeric protein of the extracellular domain of the human *Tfrc* gene and the transmembrane and intracellular domains of the mouse *Tfrc* gene was inserted into exon 2 of the mouse *Tfrc* gene.¹⁰ The hTfR-KI/*Ids*-KO double-mutant mice were obtained by crossbreeding *Ids*-KO mice with hTfR-KI mice. C57BL/6 mice were purchased from Charles River, Japan (Yokohama, Japan). All animal experiments were performed in accordance with the ARRIVE guidelines 2.0, and the protocols were approved by the Animal Care and Use Committees of JCR Pharmaceuticals (JR141-P2004). Mice were housed under 12-h light-dark cycles and freely accessed with water and a standard rodent chow diet. The animals were acclimatized for 20 days prior to the study.

Brain delivery of pabinafusp alfa

Pabinafusp alfa was intravenously administered to male MPS II (hTfR-KI/*Ids*-KO) mice (45 weeks of age) at doses of 0.1, 0.5, or 2.0 mg/kg, and brain samples were collected 8 h after the administration. One hemisphere of the brain was used for quantitative drug detection using an electrochemiluminescence assay and the other for qualitative immunohistochemistry as described previously.¹⁰ For immunohistochemistry, Biotin XX Tyramide SuperBoost Kit (Thermo Fisher Scientific) was used to enhance specific signal intensity.

Study design

Male MPS II (hTfR-KI/*Ids*-KO) mice intravenously received pabinafusp alfa at 0.1, 0.5, or 2 mg/kg of body weight through the tail vein once weekly, beginning from the age of 11 week (age at which the deposition of the substrates already began¹¹), for complete 36 weeks (Figure 1). Physiological saline was administered in the same manner as the KO control (vehicle-treated MPS II) mice. C57BL/6 mice were used as the healthy controls (WT). Fifteen animals were used per group, which was determined with reference to previous studies, including five animals for substrate measurement and remaining alive animals at the end of the test period ($n = 10$ for WT group, $n = 6$ for KO control group, $n = 8$ for 0.1 mg/kg group, $n = 7$ for 0.5 mg/kg group, and $n = 9$ for 2.0 mg/kg group) for histopathological analysis. The body weights of the animals were measured weekly prior to administration of the drug. All live mice except those in bad condition

were subjected to behavioral performance tests using CatWalk gait analysis,^{38,39} pole test,⁴⁰ Y maze,^{21,41} and Morris water maze^{11,42} at the indicated time points (Figure 1). Infusion-associated reactions occurred in some mice, but the reaction was not severe enough to stop dosing, and no mice died from hypersensitive immune reactions. Therefore, immunosuppressant treatment was not required in the present study. One week (8 days) after the last dosing, CSF was collected from the cisterna magna of the mice using a glass capillary under anesthesia. Subsequently, blood and tissues (brain, liver, spleen, and heart) were collected, as described previously.^{10,11}

Measurement of HS and DS concentrations

Quantification of HS and DS was performed using liquid chromatography-tandem mass spectrometry, as described previously.¹³ Briefly, lyophilized tissues were homogenized using a mechanical shaker (BMS-AT20TP, Bio-Medical Science, Tokyo, Japan), and the homogenate mixtures were centrifuged to obtain supernatants as samples for measurement. The samples were subjected to a methanolysis reaction at 70°C for 90 min. The centrifuged samples were mixed with a 10% ammonium carbonate solution and an internal standard (reference HS and DS mixture, each at 1,000 ng/mL, reacted with deuterated methanol). Each sample was evaporated, dissolved in ultrapure water, and loaded onto a solid-phase extraction cartridge (OASIS HLB, Waters, Milford, MA). The samples eluted from the cartridge with ethanol were evaporated, dissolved in ultrapure water, and mixed with acetonitrile to prepare for further loading. High-performance liquid chromatography (HPLC) was performed using a Shimadzu 30A HPLC system (Shimadzu, Kyoto, Japan) equipped with ACQUITY UPLC BEH Amide (Waters) with an acetonitrile gradient, and mass spectrometry was performed using a Triple Quad 5500 (AB Sciex, Framingham, MA).

Histopathology

For histopathological analysis, animals euthanized by exsanguination under anesthesia with the three types of mixed anesthetic agents (medetomidine/midazolam/butorphanol: 0.3/4.0/5.0 mg/kg) were perfused with physiological saline. Tissues (brain, liver, spleen, and heart) were collected and fixed with 10% neutral-buffered formalin. The tissues were then embedded in paraffin, sliced into 4 µm sections, and stained with H&E. In addition, immunostaining for Lamp1, Gfap, and CD68 was performed with anti-Lamp1 (Abcam, Cambridge, UK: ab24170, 1:700) rabbit polyclonal antibody, anti-Gfap (Dako, Santa Clara, CA: IR524, 1:1) rabbit polyclonal antibody, and anti-CD68 (Abcam: ab125212, 1:2,000) rabbit polyclonal antibodies as primary antibodies, respectively. Signals were visualized with EnVision + System HRP Labelled Polymer Anti-Rabbit (Dako). The specimens were graded and scored as indicated in corresponding figure legends and the footnote of Table S1. The grading was performed by another person who handled the mice.

Gait analysis

Motor coordination was assessed using the CatWalk XT automated gait analysis system (Noldus Information Technology, Wageningen, the Netherlands) in a darkened room after the 21st dose

(Figure 1).^{38,39} The walkway of the system has a glass plate (130 cm in length, 20 cm in width, and 0.5 cm in thickness) that is traversed by mice from one end to the other, toward the goal box mounted at one end of the walkway. The corridor (120 cm in length, 5 cm in width, and 15 cm in height) was set up with two black walls to limit and direct an animal's movement over the glass plate. Mice footprints were recorded using the Illuminated Footprints technology (Noldus Information Technology), in which green LED light was injected into the glass plate and was completely internally reflected, except for those areas where the mouse contacts the glass plate. Mice were placed on one end of the corridor and allowed to walk on the glass plate, while gait dynamics were recorded and analyzed using the CatWalk XT software. For each parameter, multiple (typically two or three) valid runs were used to calculate the mean value of individual animals. Trials in which the mice stopped part way in the corridor were excluded from the analysis.

Pole test

Motor coordination and agility were assessed by a pole test after the 24th dose (Figure 1).⁴⁰ The pole test was conducted with a vertical pole 60 cm in length and 1 cm in diameter, and a rough surface (wrapped with grip tape) was placed at the center of a square box (92 cm on each side and 60 cm in wall height). Each mouse was placed at the top of the pole facing down and allowed to climb down the pole. The trial was performed for a maximum of 120 s, and the time to climb down was recorded. If the mouse fell from the pole, the trial was excluded from the analysis.

Y maze test

Immediate working memory was assessed by spontaneous alternation behavior in the Y maze test after the 32nd dose (Figure 1).^{21,41} The Y maze apparatus consisted of three arms made of plastic joined in the middle to form a "Y" shape. Each arm was 43.5 cm in length and 5.5 cm in width, and the height of the walls was 12.5 cm, allowing the mouse to see distal spatial landmarks. No intermaze cues were provided. Testing was carried out under dim light conditions (<40 lx at the arm level). Mice were placed into one of the arms of the maze with their head facing the end wall and allowed to explore freely for 8 min. The number and sequence of arms entered were recorded using EthoVision XT 11.5 video tracking software (Noldus Information Technology). The percentage of spontaneous alternations was calculated by dividing the number of alternations (entries into three different arms consecutively) by the total number of possible alternations (total number of arm entries minus 2) and then multiplying by 100.⁴²

Morris water maze test

Spatial learning ability was assessed by latency to reach the hidden platform in the Morris water maze test.^{11,43} Half of the animals in each group were subjected to the test after the 34th injection, while the other half of the animals in each group were subjected after the 35th injection (Figure 1). The water maze apparatus was a circular pool with a diameter of 120 cm and a depth of 18 cm, equipped

with a transparent acrylic resin platform (2 cm below the water surface). Trials were performed as described previously.¹¹ Goal latency (the time to reach the platform) was measured for a maximum of 90 s.

Statistics

Data are presented as mean \pm SEM. Statistical analysis was conducted using KyPlot 6.0 statistics software (KyensLab). Dunnett's test was used to compare the difference between the WT or KO control group and each treatment group in substrate concentration reduction efficacy and performance in gait dynamics, pole test, and Y maze test (Table S2). For the Morris water maze test, a paired t test was used to compare the difference with the trial on day 1 within each group. Statistical significance was set at $p < 0.05$. The correlation curves of the water maze performance and HS concentrations in the CNS were fitted using nonlinear least-squares regression. Statistical analysis was not performed for histopathological analysis.

SUPPLEMENTAL INFORMATION

Supplemental information can be found online at <https://doi.org/10.1016/j.omtm.2022.05.002>.

ACKNOWLEDGMENTS

We thank Shin Nippon Biomedical Laboratories for the measurement of HS and DS concentrations and Sapporo General Pathology Laboratory for histopathological analysis. We also thank all members of the Pharmacology & Toxicology Unit, Research Division of JCR Pharmaceuticals, for their support in this study. Special thanks to Matthias Schmidt, Yuji Sato, and Saiei So of JCR Pharmaceuticals for their critical reading of the manuscript. We would also like to thank Editage (www.editage.com) for English language editing. This study was founded by JCR Pharmaceuticals.

AUTHOR CONTRIBUTIONS

H. Morimoto, T.H., H.S., and K.M. conceptualized and designed the research. H. Morimoto, H. Morioka, A.I., and R.Y. performed the research and acquired the data. H. Morimoto, H. Morioka, A.I., R.Y., T.H., and K.M. analyzed the data. K.M. wrote the manuscript.

DECLARATION OF INTEREST

H. Morimoto, H. Morioka, A.I., R.Y., T.H., H.S., and K.M. received compensation as employees of JCR Pharmaceuticals. This study was sponsored by JCR Pharmaceuticals.

REFERENCES

- Neufeld, E.F., and Muenzer, J. (2001). The mucopolysaccharidoses. In *The Metabolic & Molecular Bases of Inherited Disease*, C.R. Scriver, A.L. Beaudet, W.S. Sly, and D. Valle, eds. (McGraw Hill), pp. 3421–3452.
- Tylki-Szymańska, A. (2014). Mucopolysaccharidosis type II, Hunter's syndrome. *Pediatr. Endocrinol. Rev.* 12 (Suppl 1), 107–113.
- Wilson, P.J., Morris, C.P., Anson, D.S., Occhiodoro, T., Bielicki, J., Clements, P.R., and Hopwood, J.J. (1990). Hunter syndrome: isolation of an iduronate-2-sulfatase cDNA clone and analysis of patient DNA. *Proc. Natl. Acad. Sci. U S A* 87, 8531–8535. <https://doi.org/10.1073/pnas.87.21.8531>.
- Dvorakova, L., Vlaskova, H., Sarajlija, A., Ramadza, D.P., Poupetova, H., Hrubá, E., Hlavata, A., Bzduch, V., Peskova, K., Storkanova, G., et al. (2017). Genotype-phenotype correlation in 44 Czech, Slovak, Croatian and Serbian patients with mucopolysaccharidosis type II. *Clin. Genet.* 91, 787–796. <https://doi.org/10.1111/cge.12927>.
- Vollebregt, A.A.M., Hoogeveen-Westerveld, M., Kroos, M.A., Oussoren, E., Plug, I., Ruijter, G.J., van der Ploeg, A.T., and Pijnappel, W.W.M.P. (2017). Genotype-phenotype relationship in mucopolysaccharidosis II: predictive power of IDS variants for the neuronopathic phenotype. *Dev. Med. Child Neurol.* 59, 1063–1070. <https://doi.org/10.1111/dmcn.13467>.
- Muenzer, J., Beck, M., Eng, C.M., Giugliani, R., Harmatz, P., Martin, R., Ramaswami, U., Vellodi, A., Wraith, J.E., Cleary, M., et al. (2011). Long-term, open-labeled extension study of idursulfase in the treatment of Hunter syndrome. *Genet. Med.* 13, 95–101. <https://doi.org/10.1097/gim.0b013e3181fea459>.
- Muenzer, J., Beck, M., Giugliani, R., Suzuki, Y., Tylki-Szymanska, A., Valayannopoulos, V., Vellodi, A., and Wraith, J.E. (2011). Idursulfase treatment of Hunter syndrome in children younger than 6 years: results from the Hunter Outcome Survey. *Genet. Med.* 13, 102–109. <https://doi.org/10.1097/gim.0b013e318206786f>.
- Muenzer, J., Giugliani, R., Scarpa, M., Tylki-Szymańska, A., Jegó, V., and Beck, M. (2017). Clinical outcomes in idursulfase-treated patients with mucopolysaccharidosis type II: 3-year data from the hunter outcome survey (HOS). *Orphanet J. Rare Dis.* 12, 161. <https://doi.org/10.1186/s13023-017-0712-3>.
- Seo, J.H., Kosuga, M., Hamazaki, T., Shintaku, H., and Okuyama, T. (2021). Impact of intracerebroventricular enzyme replacement therapy in patients with neuronopathic mucopolysaccharidosis type II. *Mol. Ther. Methods Clin. Dev.* 21, 67–75. <https://doi.org/10.1016/j.omtm.2021.02.018>.
- Sonoda, H., Morimoto, H., Yoden, E., Koshimura, Y., Kinoshita, M., Golovina, G., Takagi, H., Yamamoto, R., Minami, K., Mizoguchi, A., et al. (2018). A blood-brain-barrier-penetrating anti-human transferrin receptor antibody fusion protein for neuronopathic mucopolysaccharidosis II. *Mol. Ther.* 26, 1366–1374. <https://doi.org/10.1016/j.yimthe.2018.02.032>.
- Morimoto, H., Kida, S., Yoden, E., Kinoshita, M., Tanaka, N., Yamamoto, R., Koshimura, Y., Takagi, H., Takahashi, K., Hirato, T., et al. (2021). Clearance of heparan sulfate in the brain prevents neurodegeneration and neurocognitive impairment in MPS II mice. *Mol. Ther.* 29, 1853–1861. <https://doi.org/10.1016/j.yimthe.2021.01.027>.
- Yamamoto, R., Yoden, E., Tanaka, N., Kinoshita, M., Imakiire, A., Hirato, T., and Minami, K. (2021). Nonclinical safety evaluation of pabinafusp alfa, an anti-human transferrin receptor antibody and iduronate-2-sulfatase fusion protein, for the treatment of neuronopathic mucopolysaccharidosis type II. *Mol. Genet. Metab. Rep.* 27, 100758. <https://doi.org/10.1016/j.ymgmr.2021.100758>.
- Tanaka, N., Kida, S., Kinoshita, M., Morimoto, H., Shibasaki, T., Tachibana, K., and Yamamoto, R. (2018). Evaluation of cerebrospinal fluid heparan sulfate as a biomarker of neuropathology in a murine model of mucopolysaccharidosis type II using high-sensitivity LC/MS/MS. *Mol. Genet. Metab.* 125, 53–58. <https://doi.org/10.1016/j.ymgme.2018.07.013>.
- Okuyama, T., Eto, Y., Sakai, N., Minami, K., Yamamoto, T., Sonoda, H., Yamaoka, M., Tachibana, K., Hirato, T., and Sato, Y. (2019). Iduronate-2-sulfatase with anti-human transferrin receptor antibody for neuropathic mucopolysaccharidosis II: a phase 1/2 trial. *Mol. Ther.* 27, 456–464. <https://doi.org/10.1016/j.yimthe.2018.12.005>.
- Okuyama, T., Eto, Y., Sakai, N., Nakamura, K., Yamamoto, T., Yamaoka, M., Ikeda, T., So, S., Tanizawa, K., Sonoda, H., and Sato, Y. (2020). A phase 2/3 trial of pabinafusp alfa, IDS fused with anti-human transferrin receptor antibody, targeting neurodegeneration in MPS-II. *Mol. Ther.* 29, 671–679. <https://doi.org/10.1016/j.yimthe.2020.09.039>.
- Giugliani, R., Martins, A.M., So, S., Yamamoto, T., Yamaoka, M., Ikeda, T., Tanizawa, K., Sonoda, H., Schmidt, M., and Sato, Y. (2021). Iduronate-2-sulfatase fused with anti-hTfR antibody, pabinafusp alfa, for MPS-II: a phase 2 trial in Brazil. *Mol. Ther.* 29, 2378–2386. <https://doi.org/10.1016/j.yimthe.2021.03.019>.
- Giugliani, R., Martins, A.M., Okuyama, T., Eto, Y., Sakai, N., Nakamura, K., Morimoto, H., Minami, K., Yamamoto, T., Yamaoka, M., et al. (2021). Enzyme replacement therapy with pabinafusp alfa for neuronopathic mucopolysaccharidosis II: an integrated analysis of preclinical and clinical data. *Int. J. Mol. Sci.* 22, 10938. <https://doi.org/10.3390/ijms222010938>.

18. Meikle, P.J., Brooks, D.A., Ravenscroft, E.M., Yan, M., Williams, R.E., Jaunzems, A.E., Chataway, T.K., Karageorgos, L.E., Davey, R.C., Boulter, C.D., et al. (1997). Diagnosis of lysosomal storage disorders: evaluation of lysosome-associated membrane protein LAMP-1 as a diagnostic marker. *Clin. Chem.* 43, 1325–1335. <https://doi.org/10.1093/clinchem/43.8.1325>.
19. Kondagari, G.S., Fletcher, J.L., Cruz, R., Williamson, P., Hopwood, J.J., and Taylor, R.M. (2015). The effects of intracisternal enzyme replacement versus sham treatment on central neuropathology in preclinical canine fucosidosis. *Orphanet J. Rare Dis.* 10, 143. <https://doi.org/10.1186/s13023-015-0357-z>.
20. Wolf, H., Damme, M., Stroobants, S., D'Hooge, R., Beck, H.C., Hermans-Borgmeyer, I., Lüllmann-Rauch, R., Dierks, T., and Lübke, T. (2016). A mouse model for fucosidosis recapitulates storage pathology and neurological features of the milder form of the human disease. *Dis. Model. Mech.* 9, 1015–1028. <https://doi.org/10.1242/dmm.025122>.
21. Wahl, F., Allix, M., Plotkine, M., and Boulu, R.G. (1992). Neurological and behavioral outcomes of focal cerebral ischemia in rats. *Stroke* 23, 267–272. <https://doi.org/10.1161/01.str.23.2.267>.
22. Clarke, L.A., Winchester, B., Giugliani, R., Tylki-Szymańska, A., and Amartino, H. (2012). Biomarkers for the mucopolysaccharidoses: discovery and clinical utility. *Mol. Genet. Metab.* 106, 395–402. <https://doi.org/10.1016/j.ymgme.2012.05.003>.
23. Bigger, B.W., Begley, D.J., Virgintino, D., and Pshezhetsky, A.V. (2018). Anatomical changes and pathophysiology of the brain in mucopolysaccharidosis disorders. *Mol. Genet. Metab.* 125, 322–331. <https://doi.org/10.1016/j.ymgme.2018.08.003>.
24. Tomatsu, S., Shimada, T., Mason, R.W., Montaña, A.M., Kelly, J., LaMarr, W.A., Kubaski, F., Giugliani, R., Guha, A., Yasuda, E., et al. (2014). Establishment of glycosaminoglycan assays for mucopolysaccharidoses. *Metabolites* 4, 655–679. <https://doi.org/10.3390/metabo4030655>.
25. Węgrzyn, G., Jakóbkiewicz-Banecka, J., Narajczyk, M., Wiśniewski, A., Piotrowska, E., Gabig-Cimińska, M., Kloska, A., Słomińska-Wojewódzka, M., Korzon-Burakowska, A., and Węgrzyn, A. (2010). Why are behaviors of children suffering from various neuronopathic types of mucopolysaccharidoses different? *Med. Hypotheses* 75, 605–609. <https://doi.org/10.1016/j.mehy.2010.07.044>.
26. Sato, Y., and Okuyama, T. (2020). Novel enzyme replacement therapies for neuronopathic mucopolysaccharidoses. *Int. J. Mol. Sci.* 21, 400. <https://doi.org/10.3390/ijms21020400>.
27. Valayannopoulos, V., Nicely, H., Harmatz, P., and Turbeville, S. (2010). Mucopolysaccharidosis VI. *Orphanet J. Rare Dis.* 5, 5. <https://doi.org/10.1186/1750-1172-5-5>.
28. Shapiro, E.G., Jones, S.A., and Escolar, M.L. (2017). Developmental and behavioral aspects of mucopolysaccharidoses with brain manifestations - neurological signs and symptoms. *Mol. Genet. Metab.* 122, 1–7. <https://doi.org/10.1016/j.ymgme.2017.08.009>.
29. Węgrzyn, G., Jakóbkiewicz-Banecka, J., Gabig-Cimińska, M., Kloska, A., Malinowska, M., Moskot, M., Piotrowska, E., Narajczyk, M., Banecka-Majkutewicz, Z., Banecki, B., et al. (2018). Mechanisms of neurodegeneration in mucopolysaccharidoses. In *Mucopolysaccharidoses Update*, S. Tomatsu, C. Lavery, R. Giugliani, P.R. Harmatz, M. Scarpa, G. Węgrzyn, and T. Orii, eds. (Nova Science Publishers), pp. 87–113.
30. Sharma, J., di Ronza, A., Lotfi, P., and Sardiello, M. (2018). Lysosomes and brain health. *Annu. Rev. Neurosci.* 41, 255–276. <https://doi.org/10.1146/annurev-neuro-080317-061804>.
31. Stapleton, M., Kubaski, F., Mason, R.W., Yabe, H., Suzuki, Y., Orii, K.E., Orii, T., and Tomatsu, S. (2017). Presentation and treatments for mucopolysaccharidosis type II (MPS II; hunter syndrome). *Expert Opin. Orphan Drugs* 5, 295–307. <https://doi.org/10.1080/21678707.2017.1296761>.
32. Fusar Poli, E., Zalfa, C., D'Avanzo, F., Tomanin, R., Carlessi, L., Bossi, M., Rota Nodari, L., Binda, E., Marmiroli, P., Scarpa, M., et al. (2013). Murine neural stem cells model Hunter disease in vitro: glial cell-mediated neurodegeneration as a possible mechanism involved. *Cell Death Dis.* 4, e906. <https://doi.org/10.1038/cddis.2013.430>.
33. Zalfa, C., Verpelli, C., D'Avanzo, F., Tomanin, R., Vicidomini, C., Cajola, L., Manara, R., Sala, C., Scarpa, M., Vescovi, A.L., and De Filippis, L. (2016). Glial degeneration with oxidative damage drives neuronal demise in MPSII disease. *Cell Death Dis.* 7, e2331. <https://doi.org/10.1038/cddis.2016.231>.
34. Patel, P., Suzuki, Y., Tanaka, A., Yabe, H., Kato, S., Shimada, T., Mason, R.W., Orii, K.E., Fukao, T., Orii, T., and Tomatsu, S. (2014). Impact of enzyme replacement therapy and hematopoietic stem cell therapy on growth in patients with hunter syndrome. *Mol. Genet. Metab. Rep.* 1, 184–196. <https://doi.org/10.1016/j.ymgmr.2014.04.001>.
35. Arguello, A., Meisner, R., Thomsen, E.R., Nguyen, H.N., Ravi, R., Simms, J., Lo, I., Speckart, J., Holtzman, J., Gill, T.M., et al. (2021). Iduronate-2-sulfatase transport vehicle rescues behavioral and skeletal phenotypes in a mouse model of Hunter syndrome. *JCI Insight* 6, e145445. <https://doi.org/10.1172/jci.insight.145445>.
36. Tomita, K., Okamoto, S., Seto, T., Hamazaki, T., So, S., Yamamoto, T., Tanizawa, K., Sonoda, H., and Sato, Y. (2021). Divergent developmental trajectories in two siblings with neuropathic mucopolysaccharidosis type II (Hunter syndrome) receiving conventional and novel enzyme replacement therapies: a case report. *JIMD Rep.* 62, 9–14. <https://doi.org/10.1002/jmd2.12239>.
37. Higuchi, T., Shimizu, H., Fukuda, T., Kawagoe, S., Matsumoto, J., Shimada, Y., Kobayashi, H., Ida, H., Ohashi, T., Morimoto, H., et al. (2012). Enzyme replacement therapy (ERT) procedure for mucopolysaccharidosis type II (MPS II) by intraventricular administration (IVA) in murine MPS II. *Mol. Genet. Metab.* 107, 122–128. <https://doi.org/10.1016/j.ymgme.2012.05.005>.
38. Ritzel, R.M., Li, Y., He, J., Khan, N., Doran, S.J., Faden, A.I., and Wu, J. (2020). Sustained neuronal and microglial alterations are associated with diverse neurobehavioral dysfunction long after experimental brain injury. *Neurobiol. Dis.* 136, 104713. <https://doi.org/10.1016/j.nbd.2019.104713>.
39. Heinzel, J.C., Hercher, D., and Redl, H. (2020). The course of recovery of locomotor function over a 10-week observation period in a rat model of femoral nerve resection and autograft repair. *Brain Behav.* 10, e01580. <https://doi.org/10.1002/brb3.1580>.
40. Przybilla, M.J., Stewart, C., Carlson, T.W., Ou, L., Koniar, B.L., Sidhu, R., Kell, P.J., Jiang, X., James, J.R., O'Sullivan, M.G., and Whitley, C.B. (2021). Examination of a blood-brain barrier targeting β -galactosidase-monoclonal antibody fusion protein in a murine model of GM1-gangliosidosis. *Mol. Genet. Metab. Rep.* 27, 100748. <https://doi.org/10.1016/j.ymgmr.2021.100748>.
41. Hong, S.H., Belayev, L., Khoutorova, L., Obenaus, A., and Bazan, N.G. (2014). Docosahexaenoic acid confers enduring neuroprotection in experimental stroke. *J. Neurol. Sci.* 338, 135–141. <https://doi.org/10.1016/j.jns.2013.12.033>.
42. Sarnyai, Z., Sibille, E.L., Pavlides, C., Fenster, R.J., McEwen, B.S., and Toth, M. (2000). Impaired hippocampal-dependent learning and functional abnormalities in the hippocampus in mice lacking serotonin(1A) receptors. *Proc. Natl. Acad. Sci. U S A* 97, 14731–14736. <https://doi.org/10.1073/pnas.97.26.14731>.
43. D'Hooge, R., and De Deyn, P.P. (2001). Applications of the Morris water maze in the study of learning and memory. *Brain Res. Rev.* 36, 60–90. [https://doi.org/10.1016/s0165-0173\(01\)00067-4](https://doi.org/10.1016/s0165-0173(01)00067-4).